Indian Journal of Biotechnology
Vol. 18, April 2019, pp 108-118

Garlic extract based preparation of size controlled superparamagnetic hematite nanoparticles and their cytotoxic applications

Kalyani Rath and Shampa Sen*

Department of Biotechnology, School of Bio Sciences and Technology, Vellore Institute of Technology, Vellore 632014, Tamil Nadu, India

Received 13 April 2018; revised 12 March 2019; accepted 25 March 2019

Magnetic nanoparticles have been researched extensively recently for site specific cancer cell treatment. Typically, ultrafine, stable and biocompatible particles prepared using simple, economical and environment friendly approaches are greatly desirable. In the present study hematite nanoparticles were prepared by a semi-synthetic approach using aqueous garlic extract. The *Allium sativum* (as) prepared particles were appropriately characterized and checked for *in vitro* cytotoxic effects and hemocompatability. Well dispersed (polydispersity index 0.144), superparamagnetic (Ms: 15.677 emu/g), spherical particles possessing an average 10 nm diameter and good colloidal stability (zeta potential: -36.8 mV) were obtained. Nanoparticles displayed a UV absorption maximum at 450 nm and a characteristic peak at 587 cm^{-1} in the Infra-red (IR) spectra representing Fe-O bond. Various bioactive components present in the garlic extract could reduce the metal precursors as well as help in coating the nanoparticles. Nanoparticles exhibited negligible percentage hemolysis and concentration dependent cytotoxicity with inhibition concentration fifty percent (IC_{50}) values of 230 µg/ml, 346 µg/ml and 285 µg/ml for cell lines of colorectal cancer (HCT 116), breast cancer (MCF-7) and cervical cancer (HeLa), respectively. In contrast normal lung fibroblast MRC-5 cell line did not exhibit any apparent cytotoxicity in the studied concentration range. Hence, biocompatible magnetic nanoparticles were green synthesized for potential therapeutic application.

Keywords: Garlic extract, biocompatible, hematite, superparamagnetic, cytotoxicity, hemolysis

Introduction

In recent times superparamagnetic iron oxide nanoparticles (SPIONs) have attracted a lot of attention as target specific drug delivery agents[1]. When iron oxide nanoparticles lie in a critical size range of 15 nm they possess strikingly different physiochemical, thermal and magnetic properties than the bulk material and demonstrate superparamagnetic behaviour[2-3]. In such conditions, particles are magnetized under external field, but show zero coercivity and retentivity after the removal of external field[4]. Because of these unique properties iron oxide nanoparticles are used widely in drug delivery, hyperthermia treatment of cancer, magnetic resonance imaging (MRI) contrast agents, environmental remediation, biosensors, magnetic storage materials, magnetic separation, biocatalysts etc[5-10].

Among the different iron oxides, hematite is the most stable oxide and is known for its typical magnetic property[11]. Hematite is antiferromagnetic below a temperature of 263 K (Morin's temperature)[11], above which the magnetic domains rearrange themselves and exhibit weak ferromagnetic properties up to 955 K (Neel's temperature)[12]. In case of nano-scale hematite, temperature at which the magnetic domains undergo this transition is decreased significantly[11-12]. Magnetic properties of the particles have also found to depend on the synthesis route, size, composition and capping mechanism. Capping is very essential for nanoparticles as the nanoparticle surface atoms possess high energy and have a tendency to agglomerate which affects their overall size and functionality[13]. That is why nanoparticles are capped with various polymers, plant extract, silica, metal and metal oxides[13-14].

Iron oxide nanoparticles are normally prepared by co-precipitation, thermal decomposition, sonochemical, reverse micellar, hydrothermal, electrochemical and biological approaches[14]. Common challenges that are faced in the particle preparation are: (i) controlling the size distribution (ii) obtaining good colloidal stability (iii) production cost and (iv) waste disposal. Consequently, green synthesis of iron oxide nanoparticles using plant extracts has gained large

*Author for correspondence:
Tel: 0416-220574; Fax: 91-416-2243092/91-416-2240411
shampa.vitu@gmail.com

popularity recently. Plant extracts are not expensive, have wide availability and possess different functional groups that can help in bio-reduction and size controlled synthesis of the nanoparticles[15]. Polymers present in the extract can help in capping of the nanoparticles and improve their stability. Additionally, use of harmful chemicals and release of toxic byproducts is also decreased[15-16]. Various researchers have reported the use of plant extracts to coat the nanoparticles. Mahdavi and coworkers[16] have used *Sargassum muticum* water extract containing sulphated polysaccharides as the main reducing and capping agent for iron oxide nanoparticles. Similarly, magnetite particles were coated with carob leaf extract by Awwad and coworkers[17].

Current study focuses on preparation of magnetic hematite nanoparticles using aqueous garlic extract. Garlic extract contains antioxidants and various biopolymers possessing functional groups such as hydroxyl, carboxyl, aldehyde, amine and di-sulfide groups that can help in bioreduction of the iron precursors[18]. Components of the plant extract can help in capping and stabilization of the nanoparticles. Additionally, active ingredients present in the capping layer can enhance the therapeutic potential of the nanoparticles. Garlic is one of the oldest cultivated spice plants which have been used extensively in traditional medicine system. Garlic is well recognized for anticancer property, is a powerful antimicrobial, removes blood clot, improves the body immunity, lowers blood sugar and cholesterol[19].

Many ancient literatures have reported the external use of garlic by physicians in ancient India and Egypt for tumor treatment. Garlic intake has been shown to decrease the risk of colorectal, stomach, lung, esophageal, breast and bladder cancer[19-20]. Organosulfur compounds such as alliin, allicin, ajoene, diallyl sulphide and allixin that are present in the extract are primarily responsible for the cytototoxic property of garlic[20]. Hence, garlic extract coated hematite nanoparticles can be used as novel anticancer agents. Previously, garlic essential oil has been used by Yang and coworkers[21] as a coating agent for iron oxide nanoparticles and validated for insecticidal activity against *Tribolium castanum*. But for the first time, we have reported here the synthesis of aqueous garlic extract coated hematite nanoparticles and investigated their cytotoxic activity on four different cell lines.

Materials and Methods

Chemicals

Sodium hydroxide, ferrous sulphate and ferric chloride were of analytical grade, purchased from Merck, Germany and were used without any further purification. Garlic samples were obtained from local market, Vellore, Tamil Nadu. Cancer cell lines HCT 116, MCF-7, HeLa and MRC-5 were obtained from National Centre for Cell Science, Pune, India. All the aqueous solutions were prepared in double distilled water. Cell culture media (Rosewell Park memorial 1640 medium, Eagle's minimum essential medium, Dulbecco's Modified Eagle medium), Fetal bovine serum, MTT (3-[4,5-dimethylthiazol-2-yl]-2,5-diphenyl tetrazolium bromide) and DMSO (dimethyl sulfoxide) were obtained from HiMedia Laboratories, Bengaluru. Metformin, EDTA (ethylenediaminetetraacetic acid), Triton X, DPPH (2,2'-diphenyl-1-picrylhydrazyl) and phosphate buffer saline (PBS) were obtained ordered from Sigma Aldrich (currently Merck).

Extract Preparation and Synthesis of Hematite Nanoparticle

Synthesis of nanoparticles was obtained by using slightly modified protocol followed by Awwad *et al*. A novel microwave mediated heating was used to obtain aqueous garlic extract. About 4 g of garlic cloves were ground finely using mortar and pestle in 20 ml of distilled water. The crude extract was heated thrice using microwave (Samsung 23 L capacity) for a time period of 30 sec and 200 W power at temperature 80-100°C. The mixture was subjected to centrifugation for 10 min at 6000 rpm and thereafter filtered using Whatman filter paper 1. Garlic extract was analyzed qualitatively using standard protocols for the presence of various phyto-constituents[22]. Antioxidant activity was estimated using DPPH (2,2'-diphenyl-1-picrylhydrazyl) radical scavenging method reported elewhere[23]. In brief, 1 ml aliquot of garlic extract and various nanoparticle concentrations (200-1000 µg/ml) was taken and to it was added 4 ml ethanolic solution of DPPH. The sample was vortexed, incubated at room temperature for 30 min and subsequently, centrifuged at 10,000 rpm for 2 min. Absorbance of the supernatant was read at 517 nm and ascorbic acid was taken as the positive reference. This radical scavenging activity or percentage inhibition of free radical by DPPH was calculated by the following formula:

$$\% \text{ inhibition} = \frac{\text{Abs}_c - \text{Abs}_s}{\text{Abs}_c} \quad \ldots (1)$$

Where, Abs_c and Abs_s refer to absorbance of control and the sample respectively at 517 nm. Synthesis of iron oxide nanoparticles was carried out by co-precipitation technique using double precursor system. At first, 2:1 molar ratio of $FeCl_3$ and $FeSO_4$ were dissolved in 50 ml of water and contents were uniformly heated for 10 min. Thereafter, 10 ml of fresh garlic extract was mixed and mixture was homogenized for another 10 min. Finally, 20 ml of 2N NaOH was added and solution was shaken vigorously for 10 min. Reaction temperature was maintained at 80°C throughout the synthesis step. After completion of precipitation reaction, particles were washed thrice with distilled water, air dried and crushed properly to obtain fine powder.

Instrumentation

Optical properties of the particles were recorded using UV Visible spectrophotometer (Jenway-6305, λ = 198 - 1000 nm) provided with xenon light source. X-ray diffraction analysis was carried out with Schimadzu Smart Lab X Ray diffractometer between 10°– 90° wavelength of 1.54 Å. Cu Kα radiation was used for the purpose and set values for operation were 40 KV/30 mA. Nanoparticles were desiccated for 72 h on carbon tape, spluttered with gold and subsequently, electron microscope image was obtained using scanning electron microscope (Zeiss Ultra 55, Germany). Elemental composition was also found using the EDS (energy dispersive spectrophotometry) system provided with the scanning electron microscope. Philips CM 200 transmission electron microscope operating at a voltage of 20 kV was employed for measuring the particle size. Log normal distribution of the particles and the colloidal stability was characterized using Nanopartica SZ-100 nanoparticle analyzer (Horiba Ltd., Kyoto, Japan). To confirm the presence of iron oxide and analyze the different functional groups present on the nanoparticle surface IR spectra were documented using Perkin Elmer GX FTIR in the range of 400-4,000 cm^{-1}. Magnetic behavior of the particles was studied by Lakeshore VSM 7410. Thermogravimetric measurement was done with SDT Q600, TA Instruments (USA).

Cytotoxicity Assay

Cytotoxicity assay of the nanoparticles was performed on four cell lines: human colorectal (HCT 116), breast cancer (MCF 7), cervical cancer (HeLa) and normal lung fibroblast (MRC 5) cells using slightly modified protocol given by Rajendran *et al*. Colorectal cancer HCT 116 cell lines were cultured in RPMI (Roswell Park Memorial) 1640 medium supplemented with 10% heat inactivated fetal bovine serum (FBS), while MCF 7 cell lines were cultured in Eagle's minimum essential medium (EMEM) with 10% FBS. Culture medium used for both HeLa and MRC 5 cell lines was Dulbecco's modified Eagle medium respectively supplemented with 10% FBS. Cells growing in log phase were seeded at a density of 5000 cells per well in a 96 well culture plate for 24 h at 37°C, 5% CO_2 incubator. Synthesized nanoparticles were added in concentration range of 10-320 µg/ml and incubated for 24 h followed by addition of 3-(4,5-dimethylthiazol-2-yl)-2,5-diphenyltetrazolium bromide (MTT). Stock solution of MTT was prepared by dissolving about 5 mg of MTT in 1X Phosphate buffer saline. Then it was filtered through a 0.2 µm filter and stored at 2–8°C for further use. To each well 100 µl of this solution was added and incubation was done for about 3-4 h. After incubation, MTT reagent was discarded by pipetting out without disturbing the cells. Subsequently, 100 µl of DMSO (dimethyl sulfoxide) was added rapidly to solubilize formazan, and the absorbance was read at 510 nm. DMSO 1% was taken as the negative control and 10 mM metformin was taken as positive control. Metformin is a common type 2 antidiabetic agent which has been recently established for inhibiting various types of cancer cells[24]. Metformin mainly inhibits mTORC1 (mammalian target of rapamycin complex 1) pathway which is important in cancer cell growth and development. It also activates AMP kinase activity and thereby affects mitochondrial respiration and eventually causes cell death.

Hemolysis Assay and Antioxidant Assay of Nanoparticles

Hemolysis assay is a common technique to evaluate the bio-compatibility of nanoparticles specifically, their impact on erythrocyte membrane. Different steps were performed according to the protocol outlined by Choi *et al*[25]. Goat blood samples (slaughter house, Katpadi, Vellore) were collected in tubes containing small amount of anticoagulant, EDTA. About 2 ml of blood sample was taken, appropriately diluted using 0.2 M PBS (pH 7.4) and centrifuged at 10000 rpm for 10 min at 4°C. Pellet containing RBC was washed thrice and resuspended in PBS. Different concentrations of nanoparticle (200, 400, 600, 800 and 1000 µg/ml) were prepared by dissolving the nanoparticles in PBS and subsequently sonicating them. About 100 µl of

different nanoparticle concentrations were taken and mixed with 2900 µl of blood suspended in PBS buffer. The mixture was allowed to incubate at 37°C for 1 h. After the incubation time period, the suspension was centrifuged at 5000 rpm, 5 min and absorbance of the supernatant was recorded at 550 nm. Triton X and PBS were taken as the positive and the negative control, respectively.

$$\% \text{ hemolysis} = \frac{\text{Abs}_s - \text{Abs}_{nc}}{\text{Abs}_{pc} - \text{Abs}_{nc}} \quad \ldots (2)$$

where, Abs_s, Abs_{nc}, Abs_{pc} are absorbance of sample, negative control and positive control, respectively. Antioxidant assay of HNP was performed as detailed in previous literature[23].

Results and Discussions

Phytochemical Analysis of Garlic Extract

Aqueous garlic extract obtained was pale yellow in colour (Fig. 1B). Phytochemical profile and anti-oxidant assay of the prepared extract are presented in Figure 1C & 1D, respectively. Phytochemical tests showed the presence of carbohydrate, glycosides, tannins, saponins, steroids and protein (Table 1). Antioxidant activity of the aqueous extract was measured using DPPH radical scavenging method. DPPH possesses an odd pair of electron responsible for its purple color and characteristic peak at 517 nm. Upon interaction with antioxidants, DPPH receives a hydrogen atom from the antioxidants, gets reduced and undergoes a color change to yellow. In comparison to the standard, ascorbic acid (IC 50 value: 9.11 µg/ml), the prepared extract showed an IC_{50} value of 0.74 mg/ml. With the increase in concentration of the extract, DPPH radical scavenging activity was found to increase. Results based on the DPPH assay validate the presence of antioxidants. The various antioxidants and other functional groups present in the extract can help in bioreduction of the nanoparticles. Carbohydrate, protein and glycosides can provide a surface coating and improve the nanoparticle stability.

Preparation of Nanoparticles

Figure 2A represents the formation of nanoparticles using garlic extract. Nanoparticles were synthesized by a modified co-precipitation reaction. Preliminary confirmation of the formation of the nanoparticles was done by measuring the optical properties using UV-visible spectrophotometer (Fig. 2B). The absorption peak for the synthesized particles was found at a wavelength of 450 nm, in contrast to the garlic extract which had a wavelength maxima centered at 300 nm. As reported in previous literatures absorption band in the region 330-450 nm confirms the presence of magnetic nanoparticles[26-27].

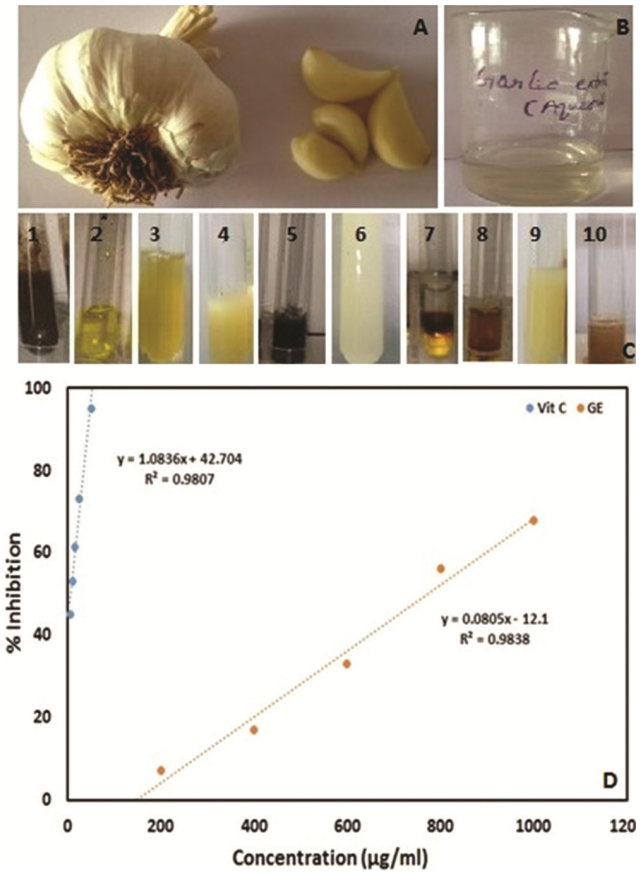

Fig. 1 — Image for (A) garlic cloves, (B) aqueous garlic extract, (C) phytochemical profile of garlic extract; where 1, 2, 3, 4, 5, 6, 7, 8, 9, 10 represent test to check presence of carbohydrate, alkaloid, flavanoid, glycosides, tannins, saponins, steroids, triterpenes, phenols, proteins, respectively and (D) antioxidant assay of garlic extract.

Table 1 — Phytochemical analysis of aqueous garlic extract

S No	Secondary metabolite	Presence/Absence
1	Carbohydrate	+
2	Alkaloid	-
3	Flavanoid	-
4	Glycosides	+
5	Tannins	+
6	Saponins	+
7	Steroids	+
8	Triterpenes	-
9	Phenols	-
10	Proteins	+

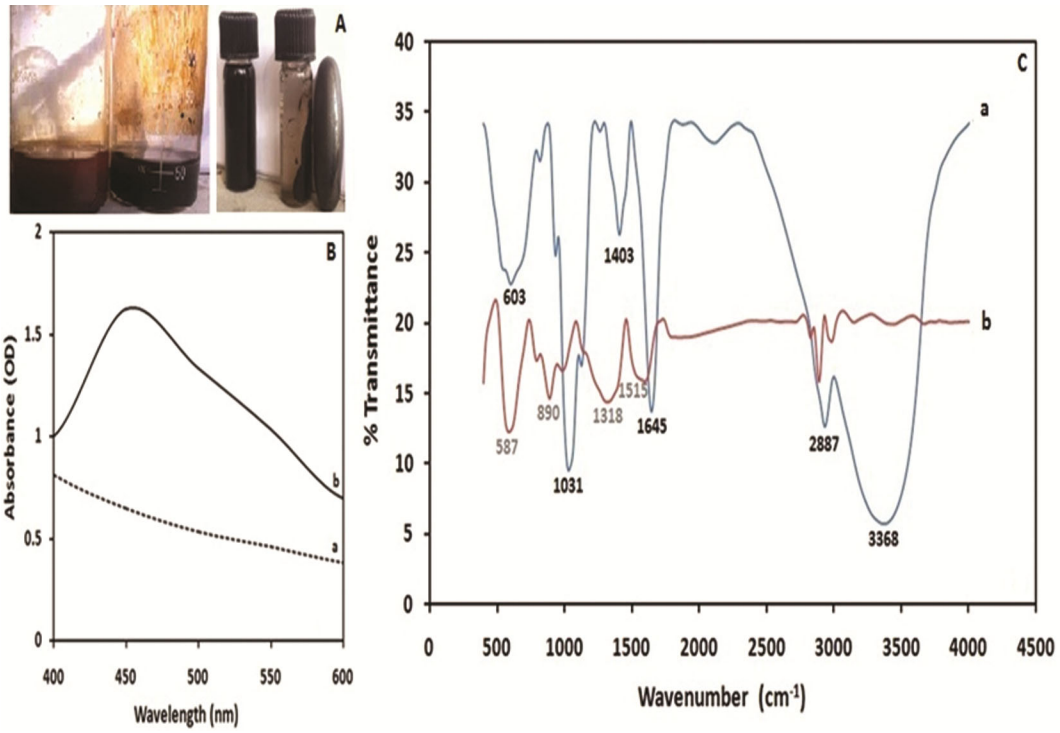

Fig. 2 — (A) Represents superparamagnetic particles obtained after completion of precipitation reaction, (B) UV-visible absorption spectra of (a) garlic extract (b) garlic-synthesized particles and (C) FTIR spectrum of (a) garlic aqueous extract (b) hematite nanoparticles.

Fourier transform infra-red (FTIR) spectra of nanoparticle and garlic extract are presented in Figure 2C. Aqueous garlic extract showed the presence of main peaks at 603 cm^{-1}, 1031 cm^{-1}, 1403 cm^{-1}, 1645 cm^{-1}, 2887 cm^{-1} and 3368 cm^{-1} which corresponded to C–H bend of alkynes, SO_2 groups of sulfones, -OH bond of carboxylate, C=O group of peptides, symmetric or asymmetric C-H bond and hydroxyl groups, respectively[28]. Nanoparticles showed the presence of strong characteristic band at 587 cm^{-1} indicating the presence of Fe-O bond, iron being present in tetrahedral site[29]. Stretching band at 3368 cm^{-1} in the garlic extract was missing in the particles indicating involvement of hydroxyl group in the bio-reduction process. Additionally, instead of two vibration bands at 1403 cm^{-1} and 1645 cm^{-1} in the extract, single overlapped band was present at 1515 cm^{-1} and a red shift in peak was observed for 1031 cm^{-1} for the synthesized particles. Further, a less intense peak observed at 810 cm^{-1} corresponding to organosulfur compounds was also altered[30]. As reported by earlier studies, alterations in IR peaks were possibly because of their involvement in the precipitation reaction. Hematite nanoparticles also demonstrated presence of additional peaks at 890 cm^{-1} and 2887 cm^{-1} denoting –NH bonds of primary amines and symmetric or asymmetric CH groups, respectively. Altogether, any shift or change in characteristic peaks for garlic extract indicated their role in green synthesis of nanoparticle, while presence of peaks for plant extract derived functional groups in IR spectrum of nanoparticle, confirmed the garlic extract based coating and stabilization of particle. Similar reduction mechanism of garlic extract and their role in nanoparticle green preparation and surface stabilization was also detailed in earlier report[31]. Based on the present findings and earlier reports, reaction mechanism of iron oxide may be described as follows: Vigorous heating of the solution containing $FeCl_3$ and $FeSO_4$ led to dissociation of the iron precursors to their ionic forms Fe^{3+} and Fe^{2+} (pH: 2-3)[32]. Addition of garlic extract (pH: 7.2) caused the reduction of ferric ions to ferrous state, while some of the ferric ions were converted to ferric hydroxide (pH: 3-4). Upon addition of sodium hydroxide to the mixture, ferrous ions interacted with atmospheric oxygen to form iron oxide hydroxide (α-FeOOH). Finally, maintenance of high temperature throughout the reaction resulted in formation of hematite phase from iron oxide hydroxide (pH of 6-7). Similar results of phase evolution have also been observed earlier[33]. Addition of ferrous ions helped in maintaining the

molar ratio needed for Fe_2O_3 synthesis. Usually, employment of 2 : 1 molar $FeCl_3/FeSO_4$ in precipitation reaction results in formation of magnetite phase (pH 12-13). But, in the present case, addition of appropriate plant extract volume at specific time resulted in hematite phase formation (pH 6-7). Reaction was highly reproducible, eco-friendly and cost effective. Stepwise representations of the different reactions hypothecated based on previous reports are listed below:

$$FeCl_3 + H_2O \rightarrow Fe^{3+} + 3Cl^- + H^+ + OH^- \quad \ldots (1)$$

$$FeSO_4 + H_2O \rightarrow Fe^{2+} + SO_4^{2-} + H^+ + OH^- \quad \ldots (2)$$

$$Fe^{3+} + GE\ (Garlic\ extract) \rightarrow Fe^{2+} \quad \ldots (3)$$

$$Fe^{3+} + 3OH^- \rightarrow Fe(OH)_3 \quad \ldots (4)$$

$$2Fe^{2+} + O_2 + 2OH^- \rightarrow 2(\alpha - FeOOH) \quad \ldots (5)$$

$$\alpha - FeOOH + Fe(OH)_3 \rightarrow Fe_2O_3 + 2H_2O \quad \ldots (6)$$

Morphology and Elemental Analysis

Scanning electron micrograph (Fig. 3) revealed spherical morphology of the particles while, nanostructures displayed mean diameter in 20-30 nm range as per the transmission electron microscopic study (Fig. 4). Generally, spherical nanoparticles are precipitated when nucleation rate per unit area is uniform[34]. But, presence of high energy electrons on the particle surface caused strong interaction and particle aggregation[35]. The EDS spectrum (Fig. 5a) showed the presence of Fe, O and C. Presence of carbon may be due to the capping by the plant biomaterials. Capping of the particles with the plant extract increases the particle stability.

Magnetic Measurements and TGA Analysis

Vibration spectrum magnetometer (VSM) was employed to analyze the magnetic properties of the hematite nanoparticle at 300 K and the results are depicted in Fig. 5B. Magnetization curve was found to be sigmoidal in nature with negligible coercivity and remenence magnetization which are typical characteristics of superparamagnetic materials. The saturation magnetization M_s was measured as 15.677 emu/g. Values of saturation magnetization for bulk magnetite is 92 emu/g and of nano powder is 68 emu/g[36]. Compared to these values saturation magnetization of the as obtained particles is low. Explanation of this can be nonmagnetic coating on the surface which leads to weakening of exchange interactions in the magnetic core and hence lowered energy of magnetization[37-38]. Previous literatures have also quoted similar results. It was reported by Mahmeda and coworkers that silica capped particle showed low saturation magnetization (6.5 Am2/kg) compared to uncapped particles (60 Am2/kg) at 300 K possibly because of small weight fraction of iron oxide present inside the shell[39]. Shan *et al* and Tsai *et al* have also obtained similar decrease in saturation magnetization for coated particles[40-41].

As presented in TG curve (Fig. 5C) nanoparticles display three weight loss steps at temperatures of 110°C, 110 - 390°C and 390 - 800°C. The first two weight loss percentages of 8.36% and 14.06% can be explained on the basis of loss of loosely attached layer of water molecules and removal of garlic extract based coating agents, respectively. This surface stabilization will help in preventing the particles

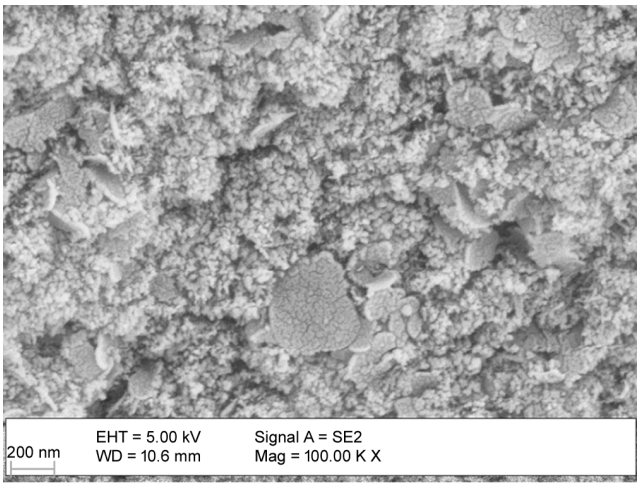

Fig. 3 — Scanning electron micrograph of hematite particles.

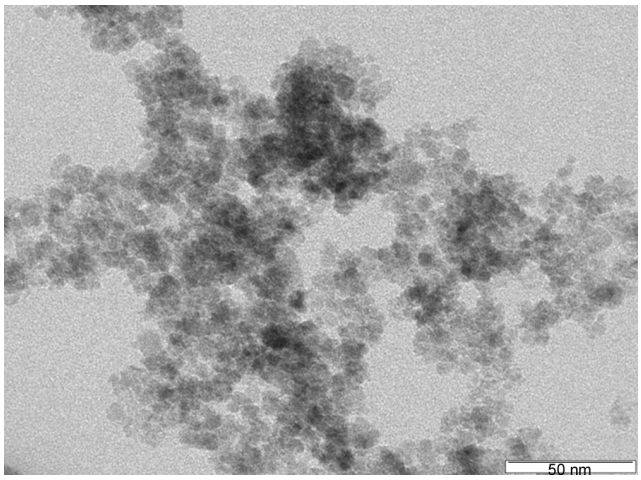

Fig. 4 — Image for TEM analysis of nanoparticles.

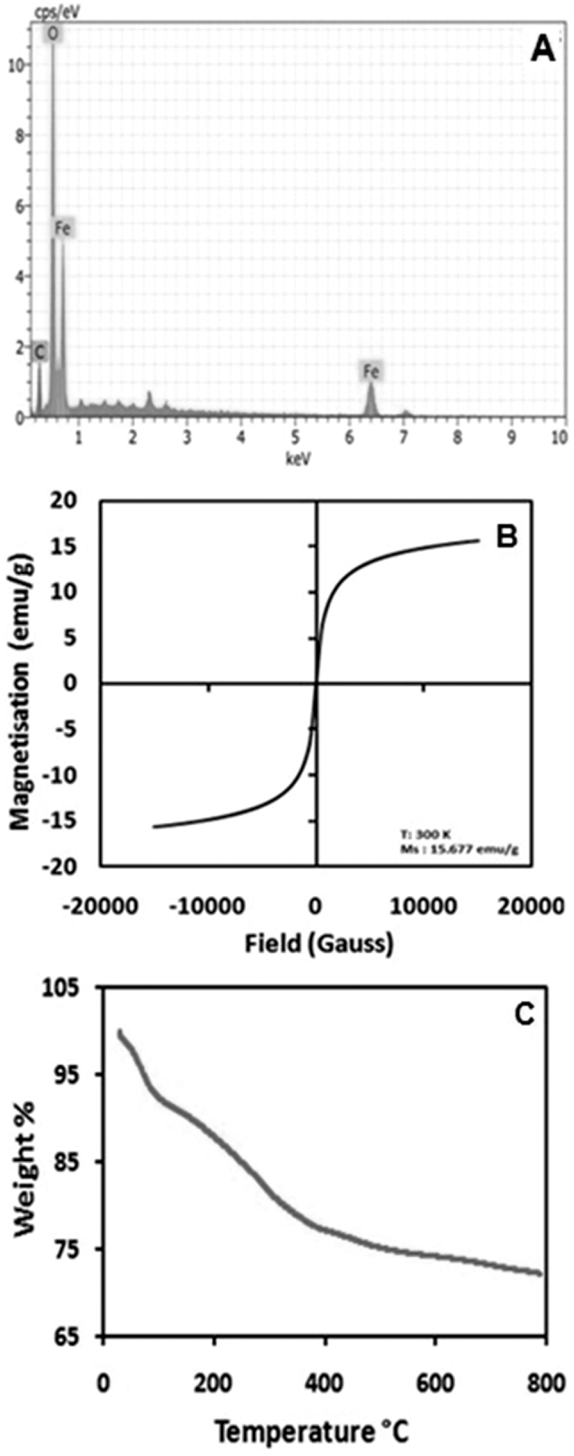

Fig. 5 — Image for (a) EDS spectrum (b) vibration spectrum magnetometer analysis and (c) Thermogravimetric measurement of hematite particles

from interacting with each other and causing large aggregate and loss of particle functionality. An additional weight loss percentage of 5.313% was also observed which may be due to the conversion of other iron oxide phase impurities to pure α-Fe_2O_3 phase[42].

X-Ray Diffraction and Dynamic Light Scattering Measurement

To investigate the crystal structure of the nanoparticles, X-ray powder diffraction analysis was performed. As shown in Figure 6A, consistent peaks were obtained at 2θ of 24.08, 33.08, 35.56, 40.8, 49.38, 54, 57.52, 62.58, 71.9 and 75.5 which can be assigned to the (012), (104), (110), (113), (024), (116), (018), (214), (1010) and (220) phase planes of hematite α-Fe_2O_3. Diffraction peaks were consistent, sharp, well resolved and matched with the hexagonal crystal structure of hematite (JCPDS file number: 33-0664). Average size of the crystals was calculated as 8 nm using Debye Scherer equation[43-44].

$$d = \frac{k\lambda}{\beta \cos\theta} \quad \ldots (7)$$

Here, d represents the particle diameter, K is the Debye Scherer constant, λ is the incident X-ray wavelength (0.15406 nm), β refers to peak width at half maximum (in radians) and θ is the angle of diffraction. Nanoparticle size distribution and stability was measured using dynamic light scattering (DLS) and are shown in Figure 6B & 6C, respectively. The particles were found to possess an average diameter of 4.4 ± 0.8 nm. The polydispersity index and zeta potential value was recorded as 0.144 and -36.8 mV, respectively. Generally, when the zeta potential value lies above a critical value of ± 25 mV, nanoparticles have good stability. Hence, as evident from the DLS measurements, nanoparticle suspension was of good colloidal stability and uniform size distribution.

Cytotoxic Studies

Garlic extract is well validated for the presence of many compounds which exhibit anticancer activity such as alliin, allicin, ajoene, diallylsulfide, allylmercaptan and allixin etc[45]. Previous studies have reported IC_{50} value of 2.5 mg/ml dry mass for fresh garlic extract on MCF7 breast cancer cell lines[46]. Also, thiacremonone, a sulphur compound found in garlic was found to exhibit an IC_{50} value of 105 µg/ml and 130 µg/ml in SW620 and HCT 116 colon cancer cell lines respectively[47]. Anticancer compounds present in the aqueous extract can form nano-conjugates and help in checking the proliferation of cancer cell lines. Hence, synthesized nanoparticles were checked for cytotoxic effects on

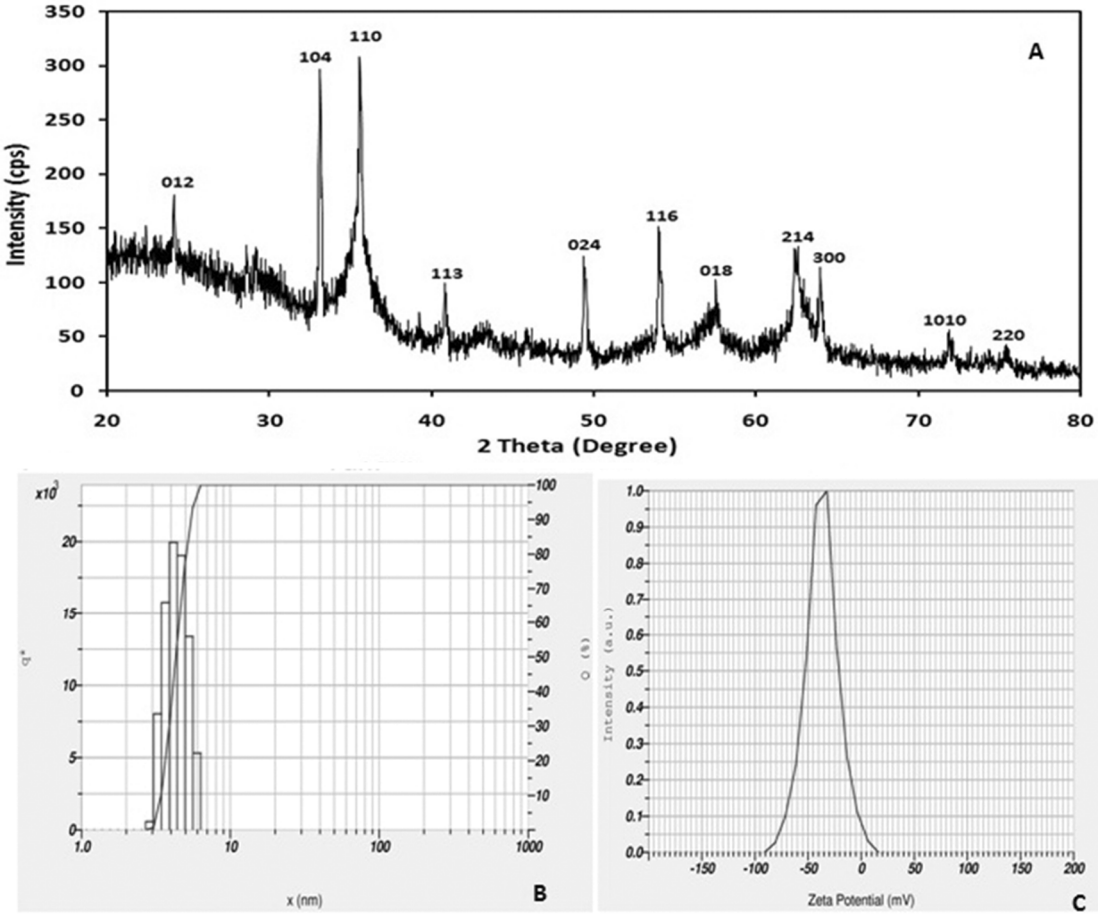

Fig. 6 — Results of (a) X ray diffraction analysis (b) hydrodynamic diameter measurement and (c) zeta potential interpretation of the as- synthesized particles.

four cell lines (HCT 116, MCF-7 and HeLa and MRC-5). As presented in Figure 7A, the as-synthesized particles exhibited a dose dependent cytotoxic response on the cancer cell lines (HCT 116, MCF 7 and HeLa) while normal MRC-5 cell lines showed ≥ 80% viability in the studied concentration range of 10- 320 µg/ml. IC_{50} values of the nanoparticles for HCT 116, MCF-7 and HeLa cell lines were 230 µg/ml, 346.25 µg/ml and 285 µg/ml, respectively. Hence, the synthesized particles exhibited slightly better cytotoxic response for human colorectal cell lines (HCT 116) followed by HeLa and MCF-7 cell lines. Role of garlic intake in colorectal cancer inhibition has been well established. Mechanism of anti-proliferative action is elaborated in Figure 7C. Reason behind normal cell lines not showing cytotoxicity effects can be on the basis of the altered structural and functional characteristics of cancer cells which allow the ingression of nanoparticles and underlying toxicity[48]. Optical images depicting the effect of the nanoparticle applications on different cell lines are presented in Figure 8.

Hemolysis and Antioxidant Assay

Nanoparticles can sometimes interfere with red blood cells by disrupting their membrane integrity. Hence for biological applications, hemolysis assay is a commonly used method to check the biocompatibility of the nanoparticles. Usually if the hemolysis percentage is < 5% nanoparticles are highly hemocompatible. For a percentage of < 10% moderate hemocompatibility is observed and particles are termed non hemocompatible if the percentage is >20%[49]. The results of hemolysis assay are shown in Figure 7B & 7D. It can be clearly seen that nanoparticles in a concentration range of 200 - 600 µg/ml show negligible hemolysis (< 5%) and are highly biocompatible. With the increase in

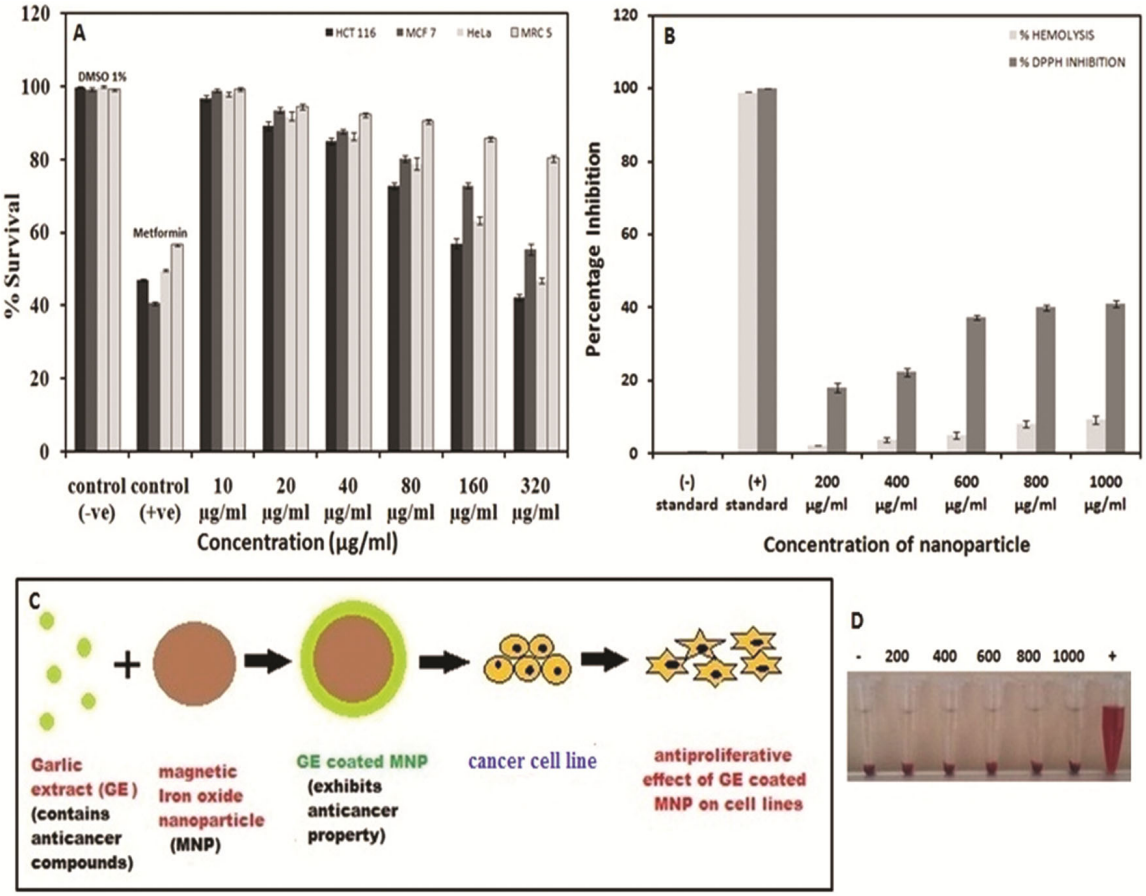

Fig. 7 — (A) Effect of nanoparticle dosages (10-320 µg/ml) on percentage survival of studied cell lines, (B) hemolysis and antioxidant assay of nanoparticle in concentration range of 200-1000 µg/ml and (C) schematic representation of cytotoxic effect of the nanoparticles, and (D) image for hemolysis assay.

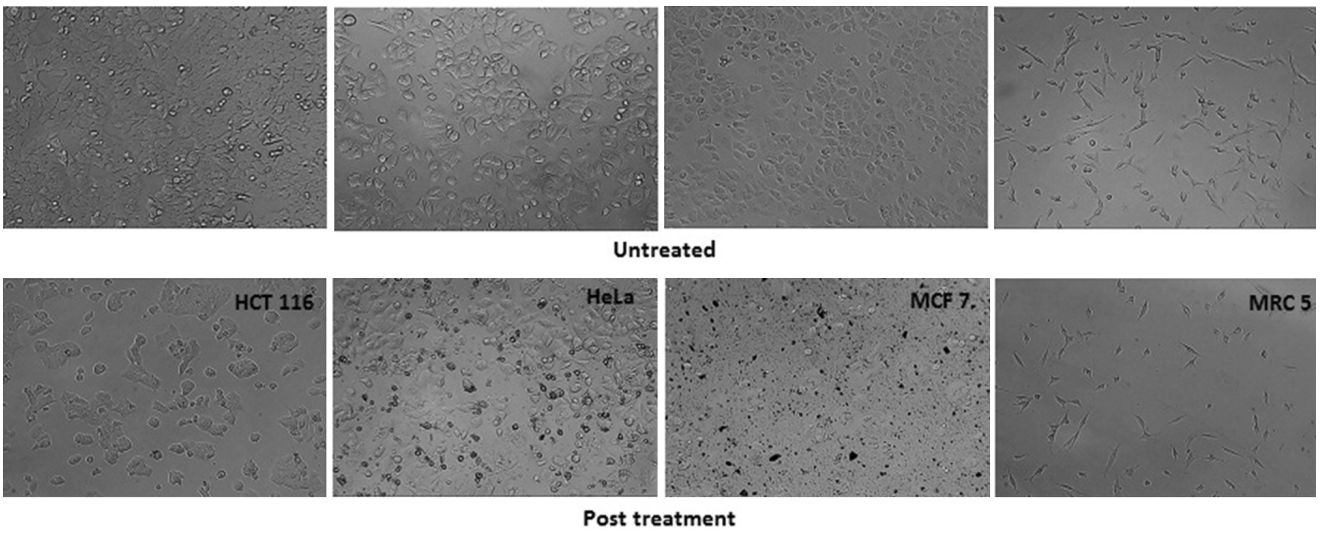

Fig. 8 — Bright field optical images showing the effect of nanoparticle treatment on the morphology of the studied cell lines (HCT 116, MCF-7 and HeLa and MRC-5).

nanoparticle dosage (600 - 1000 µg/ml) an increase in hemolysis rate is observed but it is still within the permissible limit (<10%). Hence the nanoparticles show good hemo-compatibility within the studied concentration range and can have good biological applications. Hematite particles were also tested for antioxidant activity by DPPH assay. As shown in Figure 7B, nanoparticles show a maximum of 41% DPPH inhibition at a concentration of 1000 µg/ml. Earlier researchers have also demonstrated DPPH activity of magnetic iron oxide nanoparticles. This DPPH scavenging activity may be explained on the basis of the electron transfer from the nanoparticles to the free radical in nitrogen atom of DPPH leading to decrease in absorbance at 517 nm[50].

Conclusion

In the current study, a bio synthetic approach was used to prepare hematite nanoparticles using aqueous garlic extract. Preparation protocol was simple, inexpensive, time efficient and environment friendly. After complete precipitation of the nanoparticles pH of the mixture was 6-7 in contrast to the usual 10-12 pH of the final solution. Hence byproducts of the reaction do not need any further treatment before environmental release. Nanoparticles obtained were well crystallized, stable, spherical, uniformly distributed, hemocompatible and displayed super-paramagnetic behavior. Various functional groups present in the garlic extract could coat the nanoparticles thereby increasing their stability and biocompatibility. Also because of the active anti-proliferative ingredients present in the surface layer, nanoparticles demonstrated cytotoxic effects against cancer cell lines while normal cell lines were not affected. Additionally very negligible hemolysis observed makes the synthesized particles potential candidate for applications in cancer cell treatment.

Acknowledgements

Authors are thankful to the Department of Biotechnology, SBST, VIT University, Vellore for providing the laboratory facilities. Authors are also grateful to CENSE, IISc, Bangalore for SEM, FTIR and XRD analysis.

References

1 Rajendran K, Karunagaran V, Mahanty B & Sen S, Biosynthesis of hematite nanoparticles and its cytotoxic effect on HepG2 cancer cells, *Int J Biol Macromol*, 74 (2015) 376-381

2 Sato T, Iijima T, Seki M & Inagaki N. Magnetic properties of ultrafine ferrite particles, *J Magn Magn Mater*, 65 (1987) 252-256.

3 Tartaj P, Morales M D P, Veintemillas-Verdaguer S, González-Carreño T & Serna C J, The preparation of magnetic nanoparticles for applications in biomedicine, *J Phys D: Appl Phys*, 36 (2003) 182-197.

4 Schmidt H, Nanoparticles by chemical synthesis, processing to materials and innovative applications, *Appl Organomet Chem*, 15 (2001) 331-343.

5 Laurent S, Forge D, Port M, Roch A, Robic C *et al*, Magnetic iron oxide nanoparticles: Synthesis, stabilization, vectorization, physicochemical characterizations, and biological applications, *Chem Rev,* 6 (2008) 2064-110.

6 Sunderland C J, Steiert M, Talmadge J E, Derfus A M & Barry S E Targeted nanoparticles for detecting and treating cancer, *Drug Develop Res*, 67 (2006) 70–93.

7 Ito A, Shinkai M, Honda H & Kobayashi T, Medical application of functionalized magnetic nanoparticles, *J Biosci Bioeng*, 100 (2005) 1-11.

8 Choi H, Choi S R, Zhou R, Kung H F & Chen I W, Iron oxide nanoparticles as magnetic resonance contrast agent for tumor imaging via folate receptor-targeted delivery, *Acad Radiol*, 11 (2004) 996-1004.

9 Yang H H, Zhang S Q, Chen X L, Zhuang Z-X, Xu J-G *et al*, Magnetite-containing spherical silica nanoparticles for biocatalysis and bioseparations, *Anal Chem*, 76 (2004) 1316-1321.

10 Li L, Fan M, Brown R C, Leeuwen J H V , Wang J *et al*, Synthesis, properties, and environmental applications of nanoscale iron-based materials: A Review, *Crit Rev Env Sci Technol*, 36 (2006) 405-431.

11 Bødker F, Hansen M F, Koch C B, Lefman K & Mørup S, Magnetic properties of hematite nanoparticles, *Phys Rev B*, 61 (2000) 6826-6838.

12 Schroeer D & Nininger R C, Morin transition in α-Fe2O3 microcyrstals, *Phys Rev Lett*, 19 (1967) 632-634.

13 Murad E & Schwertmann U, Temporal stability of a fine-grained magnetite, *Clays Clay Mine*r, 41 (1993) 111-113.

14 Lu A H, Salabas E L & Schüth F, Magnetic Nanoparticles: Synthesis, protection, functionalization, and application, *Angew Chem Int Ed Engl*, 46 (2007) 1222-1244.

15 Kharissova O V, Dias H V R, Kharisov B I, Pe´rez B O & Pe´rez V M J, The greener synthesis of nanoparticles, *Trends Biochem Sci*, 31 (2013) 240-248.

16 Mahdavi M, Namvar F, Ahmad M B & R Mohamad, Green biosynthesis and characterization of magnetic iron oxide (Fe_3O_4) nanoparticles using seaweed (*Sargassum muticum*) aqueous extract, *Molecules*, 18 (2013) 5954-5964.

17 Awwad A M & Salem N M. A Green and facile approach for synthesis of magnetite nanoparticles, *Nanosci Nanotech*, 2 (2012) 208-213.

18 Meriga B, Mopuri R & Krishna T M, Insecticidal, antimicrobial and antioxidant activities of bulb extracts of *Allium sativum, Asian Pac J Trop Med*, 5 (2012) 391-395.

19 Thomson M & Ali M, Garlic [*Allium sativum*]: A review of its potential use as an anti-cancer agent, *Curr Cancer Drug Targets*, 3 (2003) 67-81

20 Dausch J G & Nixon D W, Garlic: A review of its relationship to malignant disease, *Prev Med,* 19 (1990) 346-361.

21 Yang FL, Li XG, Zhu F & Lei C-L, Structural characterization of nanoparticles loaded with garlic essential oil and their insecticidal activity against *Tribolium castaneum* (Herbst) (Coleoptera: Tenebrionidae), *J Agric Food Chem*, 57 (2009) 10156-10162.

22 Harborne J B, *Phytochemical methods*, (Chapman and Hall Ltd., London), 1973

23 Brand-Williams W, Cuvelier M E & Berset C, Use of a free radical method to evaluate antioxidant activity, *Lebensm Wiss Techno1,* 28 (1995) 25-30.

24 Kasznicki J, Sliwinska A & Drzewoski J, Metformin in cancer prevention and therapy, *Ann Transl Med,* 2 (2014) 57-67.

25 Choi J, Reipa V, Hitchins V M, Goering P L & Malinauskas R A, Physicochemical characterization and in vitro hemolysis evaluation of silver nanoparticles, *Toxicol Sci*, 123(2011) 133-143.

26 Rahman O U, Mohapatra S C & Ahmad S, Fe_3O_4 inverse spinal super paramagnetic nanoparticles, *Mater Chem Phys,* 132 (2012) 196-202.

27 Islam M D S, Kusumoto Y, Kurawaki J, Abdulla-Al-Mamun M D & Manaka H A, comparative study on heat dissipation, morphological and magnetic properties of hyperthermia suitable nanoparticles prepared by co-precipitation and hydrothermal methods, *Bull Mater Sci*, 35 (2012) 1047–10.

28 Coates J, Interpretation of infrared spectra, A practical approach, in R A Meyers (Ed.), Encyclopedia of Analytical Chemistry, John Wiley & Sons publications, Chichester, 2000, 10815-10837.

29 Nunes J S, Vasconcelos C L, Cabral F A O & Fonseca J L C, Synthesis and characterization of poly(ethyl methacrylate-co-methacrylic acid) magnetic particles via miniemulsion polymerization, *Polymer*, 47 (2006) 7646-7652.

30 Rastogi Lori & Arunachalam J, Sunlight based irradiation strategy for rapid green synthesis of highly stable silver nanoparticles using aqueous garlic (*Allium sativum*) extract and their antibacterial potential, *Mater Chem Phys*, 129 (2011) 558-563.

31 El‐Refai1 A A, Ghoniem G A, El‐Khateeb A Y & Hassaan M M, Ecofriendly synthesis of metal nanoparticles using ginger and garlic extracts as biocompatible novel antioxidant and antimicrobial agents, *J Nanostructure Chem,*8 (2018) 71-81.

32 Demir A, Topkaya R & Baykl A, Green synthesis of superparamagnetic Fe_3O_4 nanoparticles with maltose: Its magnetic investigation, *Polyhedron*, 65 (2013) 282-287

33 Mascolo M C, Pei Y & Ring T A, Room temperature co-precipitation synthesis of magnetite nanoparticles in a large pH window with different bases, *Materials,* 6 (2013) 5549-5567.

34 Kim D K, Mikhaylova M, Wang F H, Kehr J, Bjelke B *et al*, Starch-coated superparamagnetic nanoparticles as MR contrast agents, *Chem Mater*, 15 (2003) 4343-4351

35 Köseoğlu Y, Alan F, Tan M, Yilgin R & Öztürk M, Low temperature hydrothermal synthesis and characterization of Mn doped cobalt ferrite nanoparticles, *Ceram Int*, 38 (2012) 3625-3634.

36 Cornell R M & Schwertmann U. The iron oxides: Structure, properties, reactions, occurences and uses, 2nd ed. (Wiley-VCH, Weinheim), 2003.

37 L F Cótica, I A Santos, E M Girotto, E V Ferri & A A Coelho, Surface spin disorder effects in magnetite and poly(thiophene)-coated magnetite nanoparticles, *J Appl Phys*, 108 (2010) 064325

38 Silva R A, Santos M J L, Rinaldi A W, Zarbin A J G, Oliveira M M *et al*, Low coercive field and conducting nanocomposite formed by Fe_3O_4 and poly(thiophene), *J Solid State Chem*, 180 (2007) 3545

39 Mahmeda N, Heczko O, Lancok A & Hannula S P, The magnetic and oxidation behavior of bare and silica-coated iron oxide nanoparticles synthesized by reverse co-precipitation of ferrous ion (Fe^{2+}) in ambient atmosphere, *J Magn Magn Mater*, 15 (2014) 353.

40 Shan Z, Yang W S, Zhang X, Huang Q M & Ye H, Preparation and characterization of carboxyl-group functionalized superparamagnetic nanoparticles and the potential for bio-applications, *J Braz Chem Soc*, 18 (2007) 1329

41 Tsai T H, Kuo L S, Chen P H, Lee D S & Yang C T, Applications of ferro-nanofluid on a micro-transformer, *Sensors*, 10, (2010) 8161.

42 M. Földvári, Handbook of the thermogravimetric system of minerals and its use in geological practice, 213th ed, (Geological Institute of Hungary, Budapest), 2011.

43 Warren B E, *X-ray diffraction*, (Dover books on Physics, Canada), 1990.

44 Cullity B D & Stock S R, *Elements of X-ray diffraction*, (Prentice hall, New Jersey), 2001.

45 Dorant E, Van den Brandt P A, Goldbohm R A, Hermus R J, and Sturmanset F, Garlic and its significance for the prevention of cancer in humans: A critical view, *Br J Cancer*, 67 (1993) 424-429.

46 Modem S, DiCarlo S E & Reddy T R, Fresh garlic extract induces growth arrest and morphological differentiation of MCF7 breast cancer cells, *Genes Cancer*, 3 (2012) 177-186.

47 Ban J O, Yuk D Y, Woo K S, Kim T M, Lee U S, Jeong *et al*, Inhibition of cell growth and induction of apoptosis via inactivation of nf-κb by a sulfurcompound isolated from garlic in human colon cancer cells, *J Pharmacol Sci*, 104 (2007) 374-383.

48 Rajendranan K, Sen S, Suja G, Senthil S L & Kumar T V, Evaluation of cytotoxicity of hematite nanoparticles in bacteria and human cell lines, *Colloids Surf B*, 157 (2017) 101-109.

49 Jiang J, Oberdorster G & Biswas P, Characterization of size, surface charge and agglomeration state of nanoparticle dispersions for toxicological studies, *J Nanopart Res*; 11 (2009) 77-89.

50 Bhattacharya K, Gogoi B, Buragohain A K & Deb P, Fe_2O_3/C nanocomposites having distinctive antioxidant activity and hemolysis prevention efficiency, *Mater Sci Eng C*, 42 (2014) 595-600.